Parasitol Res (2010) 107:39–46
DOI 10.1007/s00436-010-1830-1

ORIGINAL PAPER

Ultrastructure and molecular phylogeny of *Anisofilariata chironomi* g.n. sp.n. (Microsporidia: Terresporidia) from *Chironomus plumosus* L. (Diptera: Chironomidae)

Yuri S. Tokarev · Vladimir N. Voronin · Elena V. Seliverstova · Vyacheslav V. Dolgikh · Olga A. Pavlova · Anastasia N. Ignatieva · Irma V. Issi

Received: 28 February 2010 / Accepted: 3 March 2010 / Published online: 7 April 2010

Abstract Larvae of *Chironomus plumosus*, collected in North-Western Russia in September 2008, were infected with a microsporidium possessing broadly oval uninucleate spores in sporophorous vesicles. Sporogony and spore ultrastructure of this microsporidium differed from that of known microsporidian species, suggesting establishment of a new species, *Anisofilariata chironomi*, being a type species of a new genus. Sporogony di-, tetra-, octo-, and 16-sporoblastic. Fixed and stained spores are 4.7–6.8×3.4–5.4 μm in size, the spore measurements varying depending upon the number of spores in the sporophorous vesicle. The polaroplast is bipartite, with anterior and posterior parts composed of very thin and thick lamellae, respectively, and occupies the major volume of the spore. The polar filament is anisofilar, with two broad proximal and 10–13 narrow distal coils arranged in 2–4 layers. The sporophorous vesicle is bounded by a thin membrane and contains multiple tubular structures. Small subunit ribosomal DNA phylogeny showed basal position of the new microsporidium to a cluster uniting microsporidia infecting ciliates (*Euplotespora binucleata*), microcrustaceans (*Glugoides intestinalis*, *Mrazekia macrocyclopis*), lepidopteran insects (*Cystosporogenes* spp., *Endoreticulatus* spp.) and human (*Vittaforma corneae*), nested within Clade IV sensu Vossbrinck and Debrunner-Vossbrinck (2005 Folia Parasitol 52:131–142). No close phylogenetic relationships were found between *A. chironomi* and microsporidia from other dipteran hosts.

Y. S. Tokarev (✉) · V. V. Dolgikh · O. A. Pavlova · A. N. Ignatieva · I. V. Issi
All-Russian Institute of Plant Protection,
Russian Academy of Agricultural Sciences,
Podbelskogo sh. 3,
St. Petersburg-Pushkin 196608, Russia
e-mail: jumacro@yahoo.com

V. N. Voronin
State Research Institute of Lake and River Fisheries,
Makarova Emb. 26,
St. Petersburg 199053, Russia

E. V. Seliverstova
I.M. Sechenov Institute of Evolutionary Physiology and Biochemistry, Russian Academy of Sciences,
M. Torez ave. 44,
St. Petersburg 194223, Russia

Introduction

Microsporidia are widely distributed as parasites of animals, being most abundant in annelids, arthropods, and fishes. As many as 51 species of microsporidia belonging to 24 genera are described from chironomids, based upon morphology and ultrastructure of the developmental stages (Voronin 1999). However, no ribosomal DNA sequences are accessible through open nucleotide databases for previously described microsporidia infecting hosts of this insect group, and molecular phylogenies of microsporidia from dipteran insects are restricted to the parasites of blood-sucking mosquitos Culicidae, blackflies Simulidae (Vossbrinck et al. 2004; Andreadis 2007; Simakova et al. 2008), sandflies Phlebotominae (Cheney et al. 2000), and fruit flies Drosophilidae (Franzen et al. 2006). Most representatives of microsporidian genera infecting blood-sucking mosquitos join the *Amblyospora* clade of presumably monophyletic origin (Vossbrinck et al. 2004). Since chironomid larvae occupy the habitat similar to that of culicid larvae, a molecular phylogenetic study of microsporidia infecting hosts of both families might provide

valuable information on possible evolutionary/ecological relationships between these parasite groups.

In the present paper, we describe a new species and a new genus of a microsporidium infecting *Chironomus plumosus* larvae and provide DNA sequence analysis of this parasite.

Materials and methods

The infected midge larvae of *C. plumosus* L. (Diptera: Chironomidae) were collected in the Pobednoe Lake, Vyborg District of Leningrad Region (60°21′64″N, 29º25′ 86″E), in September of 2008. For conventional light microscopy (LM), smears of infected insect tissues were fixed with methanol and stained with Giemsa. For fluorescent microscopy, Giemsa-stained slides were additionally treated with 5 μM aqueous 4′,6-diamidino-2-phenylindole (DAPI) solution for 5 min. Digital images were acquired using Carl Zeiss Axio 10 Imager M1 equipped with epifluorescence and a digital camera. Measurements of spores were performed with Carl Zeiss Axiovision software v4.4.6. Statistical analysis was performed using *t* test, independent, by variables, with Statistica for Windows v7.0 (StatSoft, Inc.)

For transmission electron microscopy (TEM), infected tissue pieces were fixed with 2.5% glutaraldehyde solution in 0.1 M cacodylate buffer with 4% sucrose for 1–2 h and postfixed with 1% cacodylate-buffered osmium tetroxide for 1 h. Tissues were dehydrated in an ascending ethanol series and absolute acetone and embedded into epon-araldite resin. Ultrathin sections were cut using Ultracut (Reichert) and stained with 2% uranylacetate in 50% ethanol and lead citrate for 10–20 min. The material was examined using electron microscope JEM-100 CX II at an accelerating voltage of 80 kV.

For rDNA amplification and sequencing, two infected midge larvae (one deep-frozen and one ethanol-fixed) were used as independent samples. The samples were homogenized with a plastic pestle in 100 μl lysis buffer, containing 2% CTAB, 1.4 M NaCl, 100 mM EDTA, 100 mM Tris–Cl (pH 8.0). After homogenization, aliquots of 500 μl lysis buffer as above with addition of 0.2% β-mercaptoethanol and 10 μl proteinase K (20 mg mL^{-1}) were added and the samples were incubated at 65°C for 3 h. DNA was extracted routinely with phenol–chloroform (Sambrook et al. 1989) and resuspended in 50 μl UHQ water. To amplify the small subunit (SSU) rRNA gene of microsporidia, universal microsporidia primers V1f 5′-CACCAGGTTGATT CTGCCTGAC-3′ (Weiss et al. 1994) and ss1492r 5′-GGTTACCTTGTTACGACTT-3′ (Weiss and Vossbrinck 1999) were used.

PCR was run using a Bio-Rad iCycler in 20 μl volume containing 5 μl DNA template; PCR buffer; dNTPs, 0.25 mM; Taq-polymerase (Sileks, Russia), 1 U; forward and reverse primers (Evrogen, Russia), 1 pM each. A first cycle of denaturation was carried out at 92°C for 3 min, and a last cycle of extension was carried out at 72°C for 10 min. Samples were amplified for 30 cycles of denaturation at 92° C for 30 s; annealing at 54°C for 30 s; and elongation at 72°C for 30 s. The PCR products demonstrating the size about 1,200 bp were gel purified and cloned into pAL–TA vector (Evrogen, Russia). The resulting plasmids, purified with phenol–chloroform, were sequenced in both directions using M13F and M13R or V1f and ss1492r primers, with identical results for the two infected insect samples.

Newly obtained rDNA sequence, submitted to GenBank under accession number GU126383, was compared to those available in NCBI using the built-in BLAST utility (www.ncbi.nlm.nih.gov/Blast.cgi). The alignment of the newly obtained sequence with those showing significant homology (Table 1) was done automatically using CLUSTAL W algorithm and edited by eye in BioEdit v7.0.8.0 (Hall 1999). Regions containing gaps and ambiguous sites were removed, leaving an alignment of 1,088 bp length. The number of parsimony informative characters was 348.

Table 1 List of microsporidian species used in the molecular phylogeny study of *Anisofilariata chironomi* (in bold letters)

Microsporidia species	Host	Accession #
Anisofilariata chironomi	*Chironomus plumosus* (Diptera: Chironomidae)	GU126383
Cystosporogenes operophterae	*Operophtera brumata* (Lepidoptera: Geometridae)	AJ302320
Enterocytozoon bieneusi	*Macaca mulatta* (Primates: Cercopithecidae)	AF023245
Endoreticulatus bombycis	*Bombyx mori* (Lepidoptera: Bombycidae)	AY009115
Euplotespora binucleata	*Euplotes woodruffi* (Spirotrichea: Euplotidae)	DQ675604
Glugoides intestinalis	*Daphnia magna* (Crustacea: Branchiopoda)	AF394525
Liebermannia dichroplusiae	*Dichroplus elongatus* (Orthoptera: Acrididae)	EF016249
Mrazekia macrocyclopis	*Macrocyclops albidus* (Copepoda: Cyclopidae)	FJ914315
Nucleospora salmonis	*Oncorhynchus tshawytscha* (Pisces: Salmonidae)	AF185992
Orthosomella operophterae	*Operophtera brumata* (Lepidoptera: Noctuidae)	AJ302317
Vittaforma corneae	*Homo sapiens* (Primates: Hominidae)	U11046

Phylogenetic reconstructions were carried out with Bayesian Inference (BI) using MrBayes v3.1.2 (Ronquist and Huelsenbeck 2003) and Maximum Likelihood (ML) using PAUP* v4.0 β 10 (Swofford 2003), following the approach of Refardt et al. (2008). ML and BI settings were selected using jModelTest v0.1.1 (Posada 2008) by AIC (suggesting the use of the TrN+I+G model) and BIC (suggesting the TrN+G model), respectively.

MrBayes was run for 100,000 generations, and every 100th generation was sampled. The first 25% of samples was discarded as burn-in; parameter values were summarized, and a consensus tree was constructed. Standard deviation of split frequencies, which estimates the precision of the clade probabilities, reached 0.008 after 100,000 generations. Tree search in PAUP* was done heuristically with random stepwise addition (10 replicates) and TBR branch swapping. A majority rule consensus tree was calculated from 100 bootstrap replicates.

Results and discussion

Light microscopy

White hypertrophied adipose tissue, adjacent to the gut, could be seen through the transparent body covers of the infected larvae of *C. plumosus* (Fig. 1). Fresh smears of the infected adipose tissue (Fig. 2) demonstrated multiple spores in sporophorous vesicles (SPV) (Fig. 3). Studies by LM showed presence of sporogonial stages on the Giemsa-stained smears (Figs. 3, 4, 5, 6, 7, 8, 9). The earliest sporogonial stage is a meront–sporont transitional stage being an oval cell 5 μm in diameter with a densely stained cytoplasm and a diplokaryon occupying considerable volume of the cell (Fig. 4). These transitional developmental stages give rise to multinucleate sporogonial plasmodia, being oval cells 15×13 μm in size with densely stained cytoplasm and separate bright pinkish nuclei. The latter possesses a crumbly appearance due to DNA material aggregated into chromosomes, indicative of meiosis (Fig. 5). The sporoblasts are densely stained cells, round, 5–6 μm in size, or oval, 5.2–5.7×6.1–6.7 μm in size (Fig. 6). The number of sporoblasts, originating from one sporont, is divisible by two. SPVs containing four or eight spores are observed on the smears most often, though in some light fields, SPVs with 2, 12, or 16 spores are prevailing. The lumen between the SPV sheath and the spores is stained deep blue (Fig. 7).

Spores are uninucleate (see below), their shape may vary being oval to broadly oval or nearly round (Figs. 7, 8, 9). Posterior vacuole, occupying a quarter of the spore volume, is observed in the fresh spores (Fig. 3). Spore dimensions differ depending upon the number of spores in the SPV. When 12 and more spores are formed (case 1), they are 4.9–6.8×3.4–5.1 μm in size (the mean value 6.0×4.2 μm), the spore index (length to width ratio) is 1.4 (fixed and stained, n=50). When the SPV contains a lesser amount of spores (case 2), the latter are 4.7–6.7×3.4–5.4 μm in size (the mean value, 5.8×4.4 μm), the spore index is 1.3 (fixed and stained, n=50). The spore measurements (including width, length, and spore index) were statistically different (p<0.01) between case 1 and case 2. It can be concluded, that the presence of 12 and more spores in the SPV makes the spores become longer and thinner as compared to the SPVs with lesser amount of spores. However, live spores, measured 5.5–6.4×3.8–5.0 μm (n=50), do not express significant dimension differences depending upon the number of spores per SPV.

Large proportion of discharged spores is found on the fixed smears, as well as spores in the early phase of extrusion with anchoring disc protruded from the spore. Subapical position of the anchoring disc is obvious in these spores (Figs. 8, 9).

The interior of the spore is evenly stained with Giemsa, and the nuclear apparatus is not visualized. However, application of DAPI clearly demonstrates the single nucleus within the spore (Fig. 10). Aspecific DAPI binding to other components of the spore, namely the cytoplasm and the exospore, allow differentiation of the unstained zone of endospore in the intensively stained spores (Fig. 11).

Electron microscopy

TEM failed to demonstrate prespore stages of this microsporidium, so ultrastructural description is restricted to the spore and SPV morphology. On ultrathin sections, spores are ovoid or pyriform with a dense cytoplasm and a single nucleus (Figs. 12, 13). The anchoring disc is a mushroom-like structure, 350 nm in diameter, located slightly subapically or in the center of the anterior pole of the spore. The polar sac covers the anterior part of the polaroplast and protrudes towards the lateral sides of the spore by 0.5–0.7 μm (Fig. 14). The polaroplast occupies the interior two thirds of the spore or more, lying eccentrically in respect of the long axis of the spore. The polaroplast is bipartite, both parts being lamellar (Fig. 12). The anterior part of the polaroplast is composed of lamellae that are 10 nm thick and is bounded by a thin membrane, which appears as a continuation of the polar sac and breaks at the border of anterior and posterior parts. The latter is composed of lamellae 40 nm thick (Fig. 14). The polar filament is anisofilar possessing 12–15 coils. The diameter of two proximal coils measured approximately 150 nm, while the distal 10–13 coils tapered to approximately 90 nm, being arranged in 2–4 layers (Figs. 15, 16). The angle between the first proximal coil and the long axis of the spore is 30°.

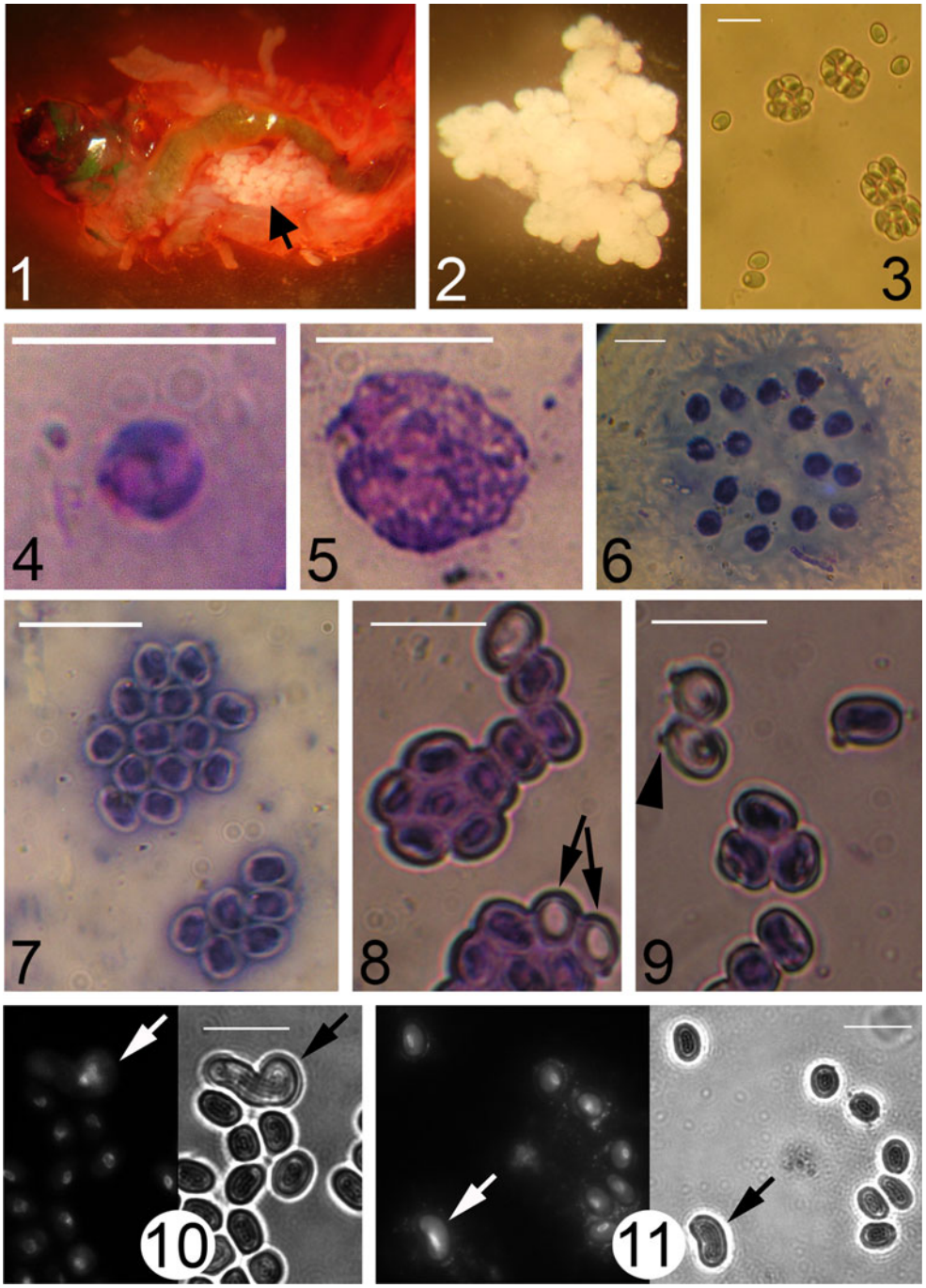

Figs. 1–11 Gross pathology of *Chironomus plumosus* and light microscopy of *Anisofilariata chironomi*. **1** *C. plumosus* larva with swelled microsporidia-infected adipose tissue (*arrow*) seen through the transparent body covers. **2** A piece of the microsporidia-infected adipose tissue. **3** Fresh spores of *A. chironomi*. **4–9** Microsporidian meront-sporont transitional stage (4), sporogonial plasmodium (5), sporoblasts (6) and spores (7–9) on Giemsa-stained smears. Some spores are empty (*arrows*) or demonstrate extruded anchoring disc (*arrowhead*). **10–11** Fluorescent (*left*) and bright field (*right*) images of the spores stained with DAPI. *Arrows* indicate atypical spores. Scale bars=10 μm

The nucleus is oval, 80–100×100–120 nm in size, lying in the central part of the spore. The nucleoplasm is of low electron density. On some sections, the nucleus is surrounded by, or adjacent to, a homogenous material of unclear nature (Figs. 12, 16, 23).

The spore wall consists of 50 nm thick electron-dense exospore and an electron-transparent endospore of 70 nm (average). In some spores, the spore wall thickness is even (Figs. 12, 15), while in others, the spore wall undulates as the exospore, and the endospore thickness changes in the range of 20–80 and 40–180 nm, respectively (Figs. 13, 14, 16). On the spore apex, the endospore narrows to 20 nm (Figs. 13, 14).

On transverse sections, the SPV bounded by 20 nm thick membrane contains 2–16 spores (Fig. 17). Multiple tubular structures 80–100 nm in diameter, limited by membranes 20–40 nm thick, are scattered unevenly in the SPV lumen or accumulated under the SPV membrane (Figs. 18, 19, 20). Sometimes, larger vesicle-like structures, 150–230 nm in diameter, are observed along with the tubular inclusions (Fig. 21). From the outer surface, the SPVs are surrounded by vesicles usually 140–200 nm in diameter, bounded by

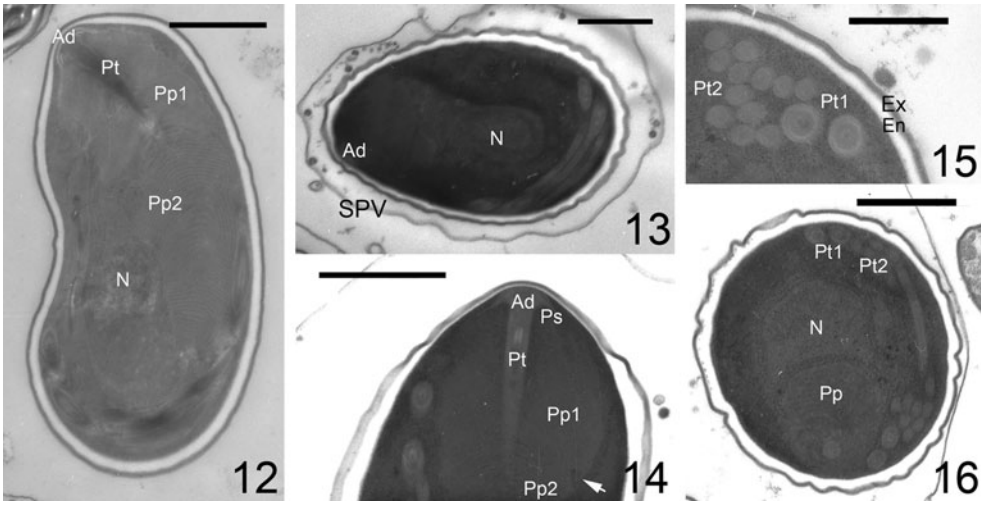

Fig. 12–16 Electron microscopy of *Anisofilariata chironomi* spores. **12** A spore with anchoring disc (*Ad*), polar filament (*Pt*), nucleus (*N*), anterior (*Pp1*), and posterior parts (*Pp2*) of the polaroplast. **13** A spore within a sporophorous vesicle (*SPV*). **14** Anterior part of the spore showing *Ad* and polaroplast surrounded by a membrane breaking at the border of *Pp1* and *Pp2* (arrow). **15** Proximal (*Pt1*) and distal coils (*Pt2*) of the anisofilar polar filament. **16** A section of the spore showing position of *N*, polaroplast and Pt coils. Scale bars=0.97 μm (12, 14, and 15) and 2.42 μm (13, 16)

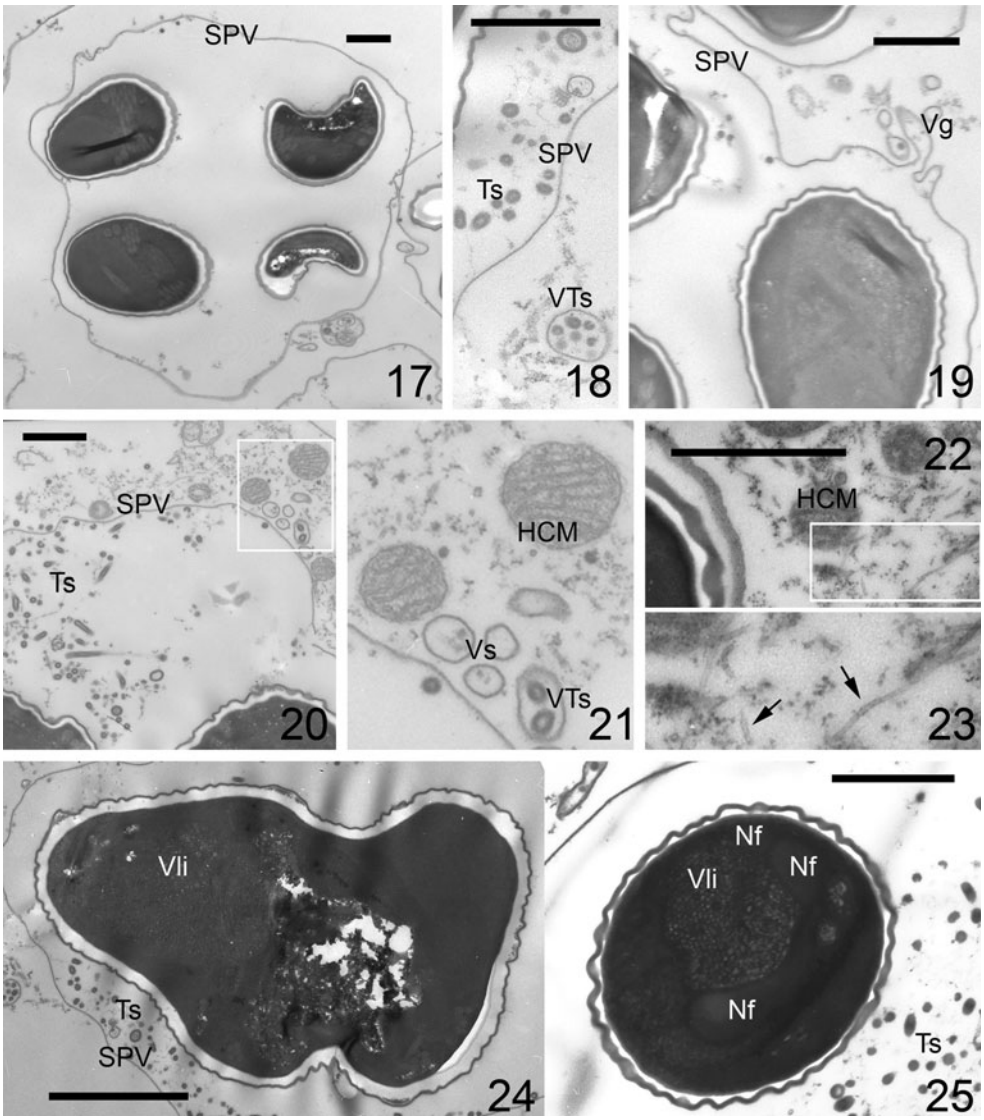

Fig. 17–25 Electron microscopy of *Anisofilariata chironomi* SPVs and teratoid spores. **17** SPV containing four spores. **18** Tubular structures (*Ts*) within the *SPV* and a vesicle with tubular structures (*VTs*). **19** Vesicles gemmating (*Vg*) from the *SPV* sheath. **20** *SPV* demonstrating tubular nature of the inclusions. **21** An enlarged detail of Fig. 20 showing host cell mitochondria (*HCM*) and vesicles adjacent to the SPV. **22** *HCM* surrounded with fine filaments in the host cell cytoplasm. **23** An enlarged detail of Fig. 22 with arrows indicating fine filaments. **24** A teratoid spore resulted from maturation of an incompletely divided sporoblast with multiple virus-like inclusions (*Vli*) in the region of polaroplast. **25** A teratoid spore with *VLi* and a fragmented nucleus (*Nf*). Scale bars= 0.97 μm (25), 1.21 μm (20, 22), and 2.42 μm (17–19, 24)

the membrane resembling that of SPV, and it can be demonstrated that these vesicles are actually gemmated from the SPV membrane (Fig. 19) and sometimes contain structures resembling the transverse sections of the tubular structures observed in the SPV lumen (Figs. 18, 19, 20, 21). Other structures often observed in the proximity of the SPVs represent, in our opinion, the host cell mitochondria. They are membrane-bound globules, 300–500 nm in diameter, with a cytoplasm of moderate density and a network of irregularly laid or parallel fine tubules running throughout the globule (Figs. 21, 22). Groups of such globules are accompanied with fine filaments 20 nm in diameter (Figs. 22, 23).

Parasite cell pathology

Irregularly shaped spores are sometimes observed on smears. They are larger than regular spores (Figs. 10, 11), sometimes possessing shape of a dividing cell with its spore wall completely formed (Fig. 10). The DAPI-stained zone corresponding to the nuclear apparatus in these spores is obviously larger as compared to the nuclei of normal spores (Figs. 10, 11). These LM observations correspond to the atypical spores found on ultrathin sections. Major volume of these spores is occupied with a compartment tightly packed with some electron-translucent virus-like particles. An example of abnormally developing spore (obviously resulted from unsuccessful sporoblast division) is associated with prominent accumulation of such inclusions in the region of polaroplast (Fig. 24), while another spore with the aforementioned inclusions bears a teratoid nucleus fragmented into several parts (Fig. 25). These observations are indicative of abortive sporogenesis, which is sometimes observed in microsporidia and is explained by various reasons. Incomplete divisions of *Enterocytozoon bieneusi* sporonts with formation of teratoid spores happen either spontaneously (Schwartz et al. 1998) or due to the effect of antimicrosporidial drugs (Ditrich et al. 1994). Spore formation of insect microsporidia may be affected by development in a non-specific host (Solter et al. 1997) or by a cellular defense reaction accompanied with melanization of the infected host tissues (Tokarev et al. 2007). Finally, cases of formation of spores with unusual polar filament structure and with double sets of organelles are explained by influence of radionuclide and organic water pollution, respectively (Ovcharenko et al. 1998). Nature of the spore pathology observed in the newly found microsporidium is unclear to us; however, we assume that it might be due to the virus-like particle accumulation in these spores.

DNA sequence analysis

Sequencing of the SSU rDNA fragment from the newly found microsporidium produced a sequence of 1,204 bp, deposited in GenBank under accession number of GU126383. A BLAST search against GenBank found the maximal sequence similarity of 78.6% between this parasite and *Vittaforma corneae* (U11046), assigning the former to the Clade IV of microsporidia of terrestrial origin (Vossbrinck and Debrunner-Vossbrinck 2005). SSU rDNA sequences of eight closely related species of microsporidia were used for phylogenetic reconstruction with *Nucleospora salmonis* and *Enterocytozoon bieneusi* chosen as an outgroup (Table 1).

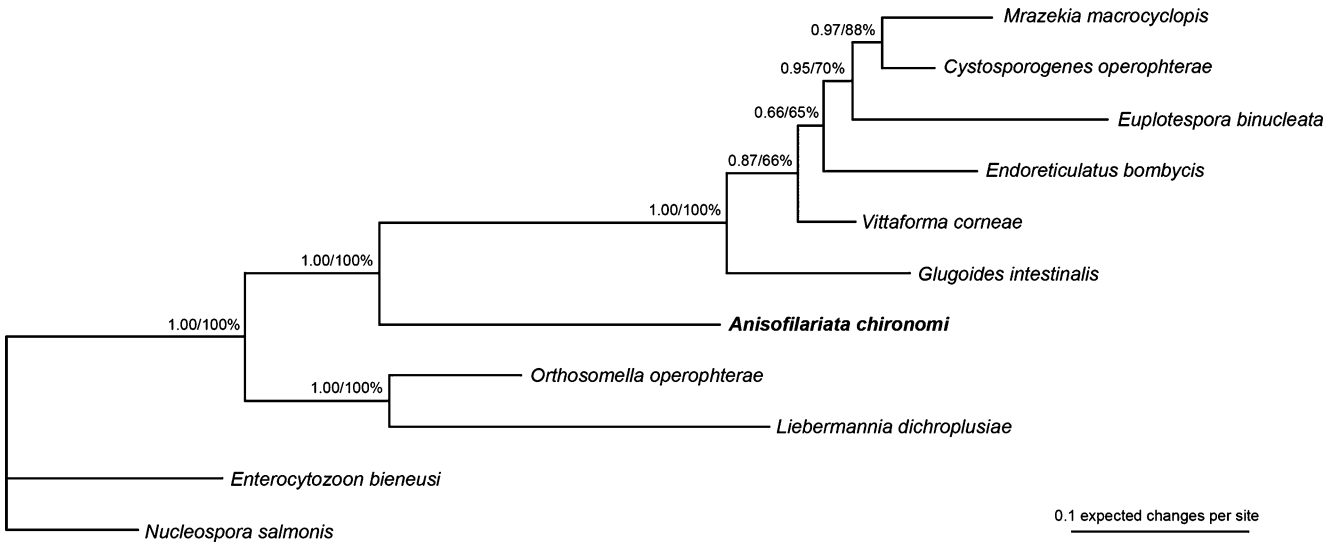

Fig. 26 Molecular phylogeny as obtained by Bayesian inference (BI) from an alignment of SSU rRNA genes of *Anisofilariata chironomi* (in *bold* letters) and ten other closely related microsporidian species. Maximum likelihood (ML) gave the identical topology. Branch support is given as probability (BI) and bootstrap value (ML)

BI and ML methods resulted in phylograms of identical topology, indicating the new microsporidium in a position basal to a cluster uniting microsporidia infecting ciliates (*Euplotespora binucleata*), microcrustaceans (*Glugoides intestinalis*, *Mrazekia macrocyclopis*), lepidopteran insects (*Cystosporogenes* spp., *Endoreticulatus* spp.), and human (*Vittaforma corneae*) (Fig. 26). No close phylogenetic relationship could be tracked between the new parasite of chironomids and other microsporidia of dipteran hosts through inspecting BLAST results and phylogenetic trees of the entire phylum of microsporidia provided by Vossbrinck and Debrunner-Vossbrinck (2005).

Differential diagnosis

Formation of several sporoblasts from one sporont in a number divisible by two or eight is typical of several genera of microsporidia (Table 2). These are *Bohuslavia* and *Larssonia* that share more common morphological characters with the newly found microsporidium than the others; and the former is also a parasite of chironomids. However, the following characters distinguish the new parasite from those previously described: a) spore formation in number divisible by two and not by four or eight, as in *Larssonia* and *Bohuslavia,* respectively, b) a polaroplast, occupying the major volume of the cell, c) anisofilar polar filament with a tilt of 30°, d) presence of vesicles gemmated from the SPV sheath on its outer side, e) secretory inclusions in the SPV lumen. Basing upon these features, we propose to establish the new genus *Anisofilariata* with the type species *Anisofilariata chironomi*, described in the present work.

Diagnosis of *Anisofilariata* gen. n.

Microsporidium is monomorphic, diplokaryotic, and monokaryotic, suggesting meiosis involvement in sporogony. Meront–sporont transitional stage possesses diplokaryotic nuclear apparatus. Sporont produces uninucleate spores in a number divisible by 2–2, 4, 8, 12, and 16. The spores are contained within a SPV and possess a bipartite polaroplast (occupying the major volume of the cell) and anisofilar polar filament (laying under an acute angle to the long axis of the spore). The SPV envelope is represented by a thin fragile membrane forming budding protrusions into the host cell cytoplasm. The SPV episporontal space contains multiple tubular inclusions. Parasites of larval adipose tissue of Chironomidae. Type species: *A. chironomi.*

Etymology The genus name reflects anisofilar polar filament, being one of the differential characters of the genus.

Diagnosis of *A. chironomi* sp. n.

Type host: *C. plumosus* L. (Diptera: Chironomidae)
Type localization: adipose tissue of the host larvae
Type locality: the Pobednoe Lake of Vyborg District, Leningrad Region, North-Western Russia (60°21′64″N, 29°25′86″E)
NCBI GenBank nucleotide accession number: *A. chironomi* (*C. plumosus*)-GU126383.

The species diagnosis corresponds to that of the genus. Spores contained within SPVs by 2–8 are broadly oval,

Table 2 Taxonomical characters of genera of microsporidia forming variable number of spores in the sporophorous vesicle (SPV)

Genus[a], host taxon	Presence of diplokaryon in transitional stage	Type of sporogonial plasmodium division	Number of spores in SPV	Polar filament	Polaroplast
Agglomerata Crustacea	No	Rosette-like	8–32	Anisofilar	Bipartite, lamellar and tubular
Agmasoma Crustacea	?	Multiple fission	8	Anisofilar	?
Alfvenia Crustacea	Yes	Multiple fission	4–8	Isofilar	Bipartite, thin and thick lamellae
Bohuslavia Insecta	Yes	Rosette-like	8–16; uniform size	Isofilar	Lamellar
Larssonia Crustacea	?	Rosette-like	8 (4–32)	Isofilar	Bipartite, lamellar
Thelohania Crustacea	Yes	Rosette-like	8	Isofilar	Bipartite, lamellar and vesicular
Trachipleistophora Mammals	No	Binary fissions	2–32	Isofilar	Lamellar
Anisofilariata Insecta	Yes	Multiple fission	4–8 (2–16); variable size	Anisofilar	Bipartite, thin and thick lamellae

[a] Taxonomical characters of genera others than *Anisofilariata* are given according to Canning and Vavra (Canning and Vavra 2000)

5.8×4.4 μm in size, while spores within SPVs containing 12 and more spores are oval, 6.0×4.2 μm in size (fixed and stained). The polaroplast is bipartite, with anterior and posterior parts composed of thin and thick lamellae, respectively. The anisofilar polar filament possesses two broad proximal and 10–13 narrow distal coils arranged in 2–4 layers.

Etymology The species name alludes to the host genus.

Acknowledgments The research is supported by the Russian Foundation for Basic Research, grants no. 07-04-00269 and 10-04-00284, and a grant from the President of Russian Federation no. MK-3419.2009.4.

References

Andreadis TG (2007) Microsporidian parasites of mosquitoes. J Am Mosq Control Assoc 23:3–29

Canning EU, Vavra J (2000) Phylum microsporida balbiani, 1882. In: Lee JJ, Leedale GF, Bradbury PC (eds) An illustrated guide of the Protozoa. Society of Protozoologists, Lawrence, KS, 1:39–126

Cheney SA, Lafranchi-Tristem NJ, Canning EU (2000) Phylogenetic relationships of *Pleistophora*-like microsporidia based on small ribosomal DNA sequences and implications for the source of *Trachipleistophora hominis* infections. J Eukaryot Microbiol 47:280–287

Ditrich O, Lom J, Dykova I, Vavra J (1994) First case of *Enterocytozoon bieneusi* infection in the Czech-Republic-comments on the ultrastructure and teratoid sporogenesis of the parasite. J Euk Microbiol 41:S35–S36

Hall TA (1999) BioEdit: a user-friendly biological sequence alignment editor and analysis program for Windows 95/98/NT. Nucl Acids Symp 41:95–98

Franzen C, Futerman PH, Schroeder J, Salzberger B, Kraaijeveld AR (2006) An ultrastructural and molecular study of *Tubulinosema kingi* Kramer (Microsporidia: Tubulinosematidae) from *Drosophila melanogaster* (Diptera: Drosophilidae) and its parasitoid *Asobara tabida* (Hymenoptera: Braconidae). J Invertebr Pathol 91:158–167

Ovcharenko M, Molloy D, Wita I (1998) Unusual polar filament structure in two microsporidia from water reservoirs with radionuclide and organic pollution. Bull Polish Acad Sci Biol 46:47–50

Posada D (2008) jModeltest: phylogenetic model averaging. Mol Biol Evol 25:1253–1256

Refardt D, Decaestecker E, Johnson PTJ, Vávra J (2008) morphology, molecular phylogeny, and ecology of *Binucleata daphniae* n. g., n. sp. (Fungi: Microsporidia), a parasite of *Daphnia magna* Straus, 1820 (Crustacea: Branchiopoda). J Eukaryot Microbiol 55:393–408

Ronquist F, Huelsenbeck JP (2003) MrBayes 3: Bayesian phylogenetic inference under mixed models. Bioinformatics 19:1572–1574

Sambrook J, Fritsch E, Maniatis T (1989) Molecular cloning: a laboratory manual. Cold Spring Harbor Laboratory, Cold Spring Harbor

Schwartz DA, Anderson DC, Klumpp SA, McClure HM (1998) Ultrastructure of atypical (teratoid) sporogonial stages of *Enterocytozoon bieneusi* (microsporidia) in naturally infected rhesus monkeys (*Macacca mulatta*). Arch Pathol Labor Med 122:423–429

Simakova AV, Vossbrinck CR, Andreadis TG (2008) Molecular and ultrastructural characterization of *Andreanna caspii* n. gen., n. sp. (Microsporida: Amblyosporidae), a parasite of *Ochlerotatus caspius* (Diptera: Culicidae). J Invertebr Pathol 99:302–311

Solter LF, Maddox JV, McManus ML (1997) Host specificity of microsporidia (Protista: Microspora) from European populations of *Lymantria dispar* (Lepidoptera: Lymantriidae) to indigenous North American Lepidoptera. J Invertebr Pathol 69:135–150

Swofford DL (2003) PAUP*. Phylogenetic analysis using parsimony (*and other methods). Version 4. Sinauer Associates, Sunderland

Tokarev YS, Sokolova YY, Entzeroth R (2007) Microsporidia-insect host interactions: teratoid sporogony at the sites of host tissue melanization. J Invertebr Pathol 94:70–73

Voronin VN (1999) The microsporidia of freshwater invertebrates and fish of Russia. The thesis of doctoral dissertation. Saint-Petersburg, 45 pp (In Russian)

Vossbrinck CR, Debrunner-Vossbrinck BA (2005) Molecular phylogeny of the Microsporidia: ecological, ultrastructural and taxonomic considerations. Folia Parasitol 52:131–142

Vossbrinck CR, Andreadis TG, Vavra J, Becnel JJ (2004) Molecular phylogeny and evolution of mosquito parasitic microsporidia (Microsporidia: Amblyosporidae). J Eukaryot Microbiol 51:88–95

Weiss LM, Vossbrinck CR (1999) Molecular biology, molecular phylogeny, and molecular diagnostic approaches to the Microsporidia. The Microsporidia and Microsporidiosis. Washington, ASM Press, pp 129–171

Weiss LM, Zhu X, Cali A, Tanowitz H B, Wittner M (1994) Utility of microsporidian rRNA in diagnosis and phylogeny: a review. Folia Parasitol 41:81–90